INSTITUTE OF PHYSICS PUBLISHING NETWORK: COMPUTATION IN NEURAL SYSTEMS

Network: Comput. Neural Syst. **13** (2002) 261–281 PII: S0954-898X(02)37530-4

# Branching rates and growth functions in the outgrowth of dendritic branching patterns

**Jaap van Pelt and Harry B M Uylings**

Graduate School Neurosciences Amsterdam, Netherlands Institute for Brain Research, Meibergdreef 33, 1105 AZ Amsterdam, The Netherlands

E-mail: j.van.pelt@nih.knaw.nl and h.uylings@nih.knaw.nl

Received 1 February 2002
Published 15 July 2002
Online at stacks.iop.org/Network/13/261

**Abstract**

The outgrowth of dendritic branching patterns proceeds by neurite elongation and branching. These actions are supported by growth cones, specialized dynamic structures at the tips of outgrowing neurites, in response to a multitude of intracellular and extracellular signals and mechanisms. Branching rates of growth cones and their temporal patterns thus reflect the extent and changes in these responses. The present study outlines a model framework to relate branching rates of individual growth cones with the growth rate of the entire dendritic tree. The branching rate of an individual growth cone is assumed to depend on the total number of growth cones at any given moment (representing competition between growth cones), on its position along the dendrite, and on a baseline component representing all other factors. Four different strategies are discussed for determining quantitatively these components from experimental data. The methods are applied in the analysis of dendritic trees of Wistar rat multipolar non-pyramidal neurons, quantitatively reconstructed at several developmental stages (Parnavelas J G and Uylings H B M 1980 *Brain Res.* **193** 373–82, Uylings H B M, Parnavelas J G, Walg H and Veltman W A M 1980 *Mikroskopie* **37** 220–4). It is shown that the baseline branching rate is a rapidly decreasing function of time, indicating the largest baseline drive for branching in the early days of outgrowth.

## 1. Introduction

During neuronal development, dendrites develop from initial protrusions from the cell body up to highly branched arborizations through a process of neurite elongation and branching. This process is mediated by growth cones, specialized structures at the terminal segments of the dendritic tree, which integrate local environmental information and intracellular signals and translate these into actions of migration and branching (splitting of a growth cone into daughter growth cones). Branching and elongation may follow different developmental patterns. For

  

instance, rat cortical pyramidal and non-pyramidal neurons show a first phase of branching and elongation up to the middle of the third postnatal week, followed by a second phase of continued elongation without branching up to at least 90 days postnatal (Parnavelas and Uylings 1980). Similar findings were obtained by Petit *et al* (1988), who recorded branching in layer V cortical pyramidal cells up to P20 and further lengthening until adulthood, and by Juraska (1982) who found no new branching after about 15 days. The first period of branching may also be followed by a period of loss of branches (regression) and subsequent regrowth as was shown in rat Purkinje cells by Pentney (1986) and in a detailed study of their terminal segment numbers by Woldenberg *et al* (1993). Remodelling of mouse Purkinje cell dendritic trees after a period of massive branching was also reported by Sadler and Berry (1984). All of these studies demonstrate a process of robust and sustained dendritic branching during the first phase of neuronal development and a rather abrupt termination of branching. Because of the principal role of growth cones in this developmental process, it is a challenging question what the experimental data, i.e., dendritic reconstructions at different developmental stages, tell us about the temporal changes in the behaviour of the individual growth cones.

Earlier studies of the dendritic branching process aimed at understanding the variations in branching pattern topology and the particular shape of the terminal segment number distributions. They showed that a dependence of the branching probability of a terminal segment on its proximal–distal position (centrifugal order) in the dendritic tree is expressed in typical probability distributions of topological tree types (e.g., Van Pelt and Verwer 1986, Van Pelt and Uylings 1999b, Dityatev *et al* 1995). Also, it was shown that a dependence of the branching probability on the momentary number of terminal segments is sensitively expressed in the shape of the terminal segment number distribution. In a number of recent studies, the shapes of observed terminal segment number distributions from a variety of cell types have accurately been described by assuming a decreasing branching probability with increasing segment number (proliferation effect) in combination with optimized values for the baseline growth rate (Van Pelt *et al* 1997, 2000, 2001, Van Pelt and Uylings 1999a, 1999b). For these studies, it was sufficient to describe the branching process as a series of consecutive branching events. Later extensions also included neurite elongation, in order to analyse the metrical properties of dendritic arborizations, such as total dendritic length and individual segment lengths. For this, however, it became necessary to include continuous time in the description of the growth process and, so far, a linear timescale has been assumed, resulting in a constant value for the baseline growth rate (e.g., Van Pelt *et al* 2000, 2001).

Because of branching, the number of growth cones participating in the growth process increases. The dendritic growth rate, i.e., the number of branching events in a dendritic tree per unit of time, thus depends on both the momentary number of growth cones and their individual branching rates. The branching rate of a growth cone is the quantitative outcome of a complex integration process of intracellular and extracellular signals and mechanisms. The individual growth cone branching rates thus may not be constant over time as, for instance, limited cellular resources are being distributed over an increasing number of growth cones, because environmental tissue develops, and because of the temporal programme of the cell itself. The need to include a proliferation-dependent component in the branching process suggests some form of competition between the increasing number of growth cones. Competition may be a general phenomenon, being expressed in, for instance, neurite outgrowth (e.g., Nowakowski *et al* 1992, Van Ooyen *et al* 2001) and in the formation of nerve connections (e.g., Van Ooyen 2001).

The lengths of individual segments are the outcomes of the joint process of growth cone elongation and branching. The temporal pattern of the branching process must therefore be expected also to have implications for segment lengths and thus the metrical properties of

the dendritic tree. The developmental approach to dendritic morphology, as discussed here, distinguishes itself from approaches in which dendritic shape is studied from the perspective of intrinsic correlations between shape characteristics. Such correlations may function as fundamental rules underlying dendritic structure and be used in sophisticated algorithms for the reconstruction of statistically realistic dendritic trees (e.g., Burke *et al* 1992, Ascoli and Krichmar 2000, Ascoli 2002).

The question addressed in this paper is whether and how the individual growth cone branching rate during dendritic development can be estimated from the observed increase in the number of dendritic segments at different developmental stages. The method, described in this paper, aims at separating the estimated branching rate into a proliferation component (competition) and a temporal pattern for the baseline branching rate component. Emphasis in the paper is given to the mathematical equations describing the branching process in terms of the competitive and baseline time-dependent component, and equations that may be helpful in analysing experimental data. The extraction of the competition parameter and the time course of the baseline growth rate is illustrated using experimental data obtained from dendritic trees of Wistar rat cortical multipolar non-pyramidal neurons at several developmental stages. These neurons are 3D reconstructed from Golgi–Cox stained tissue (Uylings *et al* 1980, Parnavelas and Uylings 1980) and analysed for their number of terminal segments. The data used in this study comprise the mean and standard deviation (SD) of the terminal segment number distributions at different time points during development.

The main finding is that the baseline branching rate is a monotonically decreasing function of time.

## 2. Branching rates and growth functions

### *2.1. Description of the branching process*

By focusing on the dendritic branching process, we may ignore the metrical properties as segment lengths and diameters. Dendritic trees will therefore be reduced to their skeletons only characterized by the number and the connectivity of the segments (topological structure). In a rooted binary tree, intermediate segments ending in bifurcation points, and terminal segments ending in terminal tips are distinguished. Segments are labelled by a centrifugal order scheme which counts the number of bifurcation points on the path from the root up to the segment. Branching is assumed to occur at terminal segments only. Although growth cones are at the head of outgrowing neurites, it may happen that after a branching event one of the daughter growth cones migrates much faster than the other one, which may even enter a ‘dormant’ state. Sooner or later, the dormant growth cone may become activated and start growing out. Then, it may be observed as if a new branch is formed along an already existing terminal segment when the faster growth cone has not yet branched. When the faster growth cone has already branched, then the new branch from a reactivated ‘dormant’ growth cone is seen as coming from an intermediate segment. Such observations are, however, very rare (e.g. Bray 1973). From a topological point of view, there is no distinction between formation of new branches at a tip of a terminal segment and formation of a new branch from a dormant growth cone along a terminal segment. A branching event in a topological tree goes with the replacement of a terminal segment by an intermediate one with a bifurcation point from which two daughter terminal segments arise. The number of terminal segments then has increased by one (figure 1). Segments maintain their centrifugal order label also when, by branching, new peripheral segments are being formed. This is in contrast to centripetal ordering schemes, when the labelling starts from the periphery towards the soma (e.g. Uylings *et al* 1975, 1986) and a relabelling is required each time a branching event occurs.

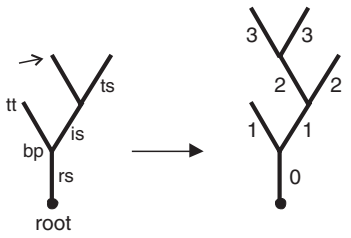


**Figure 1.** A branching event at a terminal segment (open arrow) of a dendritic tree. Terminal (ts), intermediate (is), and root (rs) segments are distinguished, as well as the root, bifurcation points (bp), and terminal tips (tt). In the resultant tree after branching, the segments are labelled according to a centrifugal ordering scheme. By branching, the number of terminal segments has been increased from 3 to 4.

### *2.2. Branching rates and growth functions*

The branching process of dendritic trees will be described in terms of the branching probabilities per unit of time of the individual terminal segments $p_s(t)$. The rate of increase in the number of terminal segments (dendritic growth rate) is then determined by both the number of terminal segments at time $t$, denoted by $n(t)$, and the branching probabilities of the individual terminal segments per unit of time $p_s(t)$ via

$$\frac{\mathrm{d}n(t)}{\mathrm{d}t} = n(t)\,p_s(t). \tag{1}$$

The growth function $n(t)$ thus results as a solution of this differential equation. Vice versa, the branching probability $p_s(t)$ can be derived from the growth function $n(t)$ via

$$p_s(t) = \frac{1}{n(t)}\frac{\mathrm{d}n(t)}{\mathrm{d}t} = \frac{\mathrm{d}\log_{\mathrm{e}} n(t)}{\mathrm{d}t}. \tag{2}$$

Although dendritic trees have an integer number of terminal segments, we will treat $n(t)$ here as a continuous differentiable real function of time, to be interpreted as the expectation value of the number of terminal segments. The branching probability of a terminal segment will be assumed to depend on three different components. The first one relates to the position of the segment in the dendritic tree, the second one relates to the total number of terminal segments in the tree, and the third one relates to all other factors. This is implemented by making the branching probability of a terminal segment $p_s(t)$ a function of the centrifugal order $\gamma$ of the terminal segment, the number of terminal segments $n(t)$, and a baseline component $D(t)$, via

$$p_s(t|n(t),\gamma) = D(t)n(t)^{-E}2^{-S\gamma}/C(t) \tag{3}$$

with parameter $E$ representing the strength of the dependence on the terminal segment number (also called the competition parameter), parameter $S$ representing the strength of the order dependence, and $C(t) = \frac{1}{n(t)}\sum_{i=1}^{n(t)} 2^{-S\gamma_i}$ being a normalization factor such that the modulation of the branching probability by centrifugal order does not change the summed branching probability for the whole tree. For the mean branching probability of a terminal segment $\bar{p}_s$ within a dendritic tree we obtain

$$\bar{p}_s(t|n(t)) = \frac{1}{n(t)}\sum_{i=1}^{n(t)} p_s(t|n(t),\gamma_i) = D(t)n(t)^{-E}. \tag{4}$$

This expression for the mean branching probability can now be inserted into equation (1) for the dendritic growth rate yielding

$$\frac{\mathrm{d}n(t)}{\mathrm{d}t} = n(t)\,\bar{p}_s(t|n(t)) = D(t)n(t)^{1-E}. \tag{5}$$

The growth rate is now expressed by two terms, one of which, $n(t)^{1-E}$, is related to the proliferation of terminal segments and shows how the growth rate depends on the momentary number of terminal segments in the tree via *competition parameter* $E$, and the other, $D(t)$, representing all other factors influencing the branching process, in the following referred to as the *baseline branching rate function* $D(t)$. By averaging the branching probability over all terminal segments, the growth function has become expressed solely in terms of the number of terminal segments without reference to the topological structures. For $E = 0$, the branching probability of an individual terminal segment does not depend on the total number of terminal segments, making the growth rate of the tree proportional to the (increasing) number of terminal segments. For $E = 1$, the branching probability of an individual terminal segment goes inversely down with the increasing number of terminal segments, making the growth rate of the tree independent of the number of terminal segments, with equation (5) reducing to

$$\frac{\mathrm{d}n(t|E=1)}{\mathrm{d}t} = D(t). \tag{6}$$

The growth function $n(t)$ is a solution of the differential equation (5). To obtain explicit solutions for the growth function we rewrite equation (5) as

$$n^{E-1}\frac{\mathrm{d}n}{\mathrm{d}t} = D(t) \tag{7}$$

and distinguish the following cases.

### *2.3. General solution of the growth function*

A solution of equation (7) can be obtained by multiplying it by $E$ (assuming $E \neq 0$)

$$En^{E-1}\frac{\mathrm{d}n}{\mathrm{d}t} \equiv \frac{\mathrm{d}}{\mathrm{d}t}n^E = ED(t), \tag{8}$$

and taking the integral over the period [0–$t$],

$$\int_0^t \frac{\mathrm{d}}{\mathrm{d}s}n^E\,\mathrm{d}s \equiv n^E|_0^t = n^E(t) - n^E(0) = n^E(t) - 1 = E\int_0^t D(s)\,\mathrm{d}s = EB(t)$$

when $n(0) = 1$ (i.e., at $t = 0$ the tree consists of one segment), resulting in

$$n^E(t) = 1 + EB(t), \qquad \text{or} \qquad n(t) = [1 + EB(t)]^{1/E}, \tag{9}$$

with $B(t)$ defined by

$$B(t) = \int_0^t D(s)\,\mathrm{d}s. \tag{10}$$

The function $B(t)$ can be interpreted as the expected number of branching events at a single terminal segment over the period [0–$t$]. Equation (9) shows how the expected terminal segment number at time $t$ depends on parameter $E$ and on $B(t)$, the time integral of function $D(t)$. Equation (9) can also be rewritten as

$$B(t) = \frac{n^E(t) - 1}{E}. \tag{11}$$

### *2.4. Particular solutions of the growth functions*

To obtain solutions for the growth function $n(t)$ we need to specify the competition parameter $E$ and the baseline branching rate function $B(t)$, as shown in equation (9). Several specific cases will be discussed. We will elaborate two specific choices for the parameter $E$, namely $E = 0$ and $E = 1$, and three specific choices for $D(t)$, namely being a constant $D$, an exponential function, or a power function.

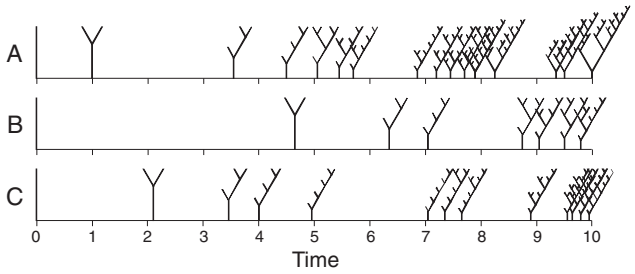


**Figure 2.** Three examples of random branching sequences when the branching probability does not depend on the momentary number of terminal segments ($E = 0$), and with parameter $D = 0.3$ (i.e., $B(10) = 3$) using this relative timescale $[0, \ldots, 10]$. Note the random occurrences of branching events, the proliferation in number of terminal segments and the different topological tree types at the end of the branching period.

*2.4.1.* Assume $E = 0$. For $E = 0$, the branching probability of a terminal segment does not depend on the number of terminal segments in the tree, and equation (7) reduces to $n^{-1}\frac{\mathrm{d}n}{\mathrm{d}t} = D(t)$, which can be rewritten as $\frac{\mathrm{d}}{\mathrm{d}t}\log_{\mathrm{e}}(n) = D(t)$, and results in a function $B(t)$:

$$B(t|E=0) = \int_0^t D(s)\,\mathrm{d}s = \int_0^t \frac{\mathrm{d}}{\mathrm{d}s}\log_{\mathrm{e}}(n(s))\,\mathrm{d}s = \log_{\mathrm{e}}(n(s))|_0^t = \log_{\mathrm{e}}(n(t)). \tag{12}$$

The solution for the growth function now becomes

$$n(t|E=0) = \mathrm{e}^{B(t)}. \tag{13}$$

*2.4.2.* Assume $E = 1$. For $E = 1$, we obtain from equation (9)

$$n(t|E=1) = 1 + B(t). \tag{14}$$

Also this equation illustrates that function $B(t)$ can be interpreted as the expected number of added segments (or branching events) up to time $t$, when the branching probability of a terminal segment is inversely proportional to the increasing number of terminal segments ($E = 1$), i.e., when the growth rate of the tree becomes independent of the proliferating number of segments.

The growth function $n(t)$ can be made explicit when specific choices are made for the baseline growth rate function $D(t)$.

*2.4.3.* Assume $D(t) = D$ to be constant. Then the baseline branching rate is independent of time, and the function $B(t)$ reduces to $B(t) = Dt$. The growth function becomes, using equation (9),

$$n(t|D) = [1 + EDt]^{1/E}, \tag{15}$$

with the specific cases

$$n(t|D, E=1) = 1 + Dt \tag{16}$$

for $E = 1$, and

$$n(t|D, E=0) = \mathrm{e}^{Dt} \tag{17}$$

for $E = 0$, using equation (13). Examples of growth sequences under the condition $E = 0$ are given in figure 2.

*2.4.4.* Assume

$$D(t) = c_1 \mathrm{e}^{c_2 t}. \tag{18}$$

When $D(t)$ is an exponential decreasing function of time we obtain for the function $B(t)$

$$B(t) = \int_0^t D(s)\,\mathrm{d}s = \int_0^t c_1 \mathrm{e}^{c_2 s}\,\mathrm{d}s = \frac{c_1}{c_2}\mathrm{e}^{c_2 t}\Big|_0^t = \frac{c_1}{c_2}[\mathrm{e}^{c_2 t} - 1] \tag{19}$$

and, using equation (9),

$$n(t|D(t) = c_1 \mathrm{e}^{c_2 t}) = [1 + EB(t)]^{1/E} = \left[1 + E\frac{c_1}{c_2}(\mathrm{e}^{c_2 t} - 1)\right]^{1/E}. \tag{20}$$

For $E = 0$, the growth function becomes, using equation (13),

$$n(t|E = 0;\, D(t) = c_1 \mathrm{e}^{c_2 t}) = \mathrm{e}^{B(t)} = \exp\left(\frac{c_1}{c_2}(\mathrm{e}^{c_2 t} - 1)\right). \tag{21}$$

*2.4.5.* Assume

$$D(t) = c_1(1 + c_2 t)^{c_3}. \tag{22}$$

For specifying the growth function $n(t)$ on the basis of this power function $D(t)$ we need to distinguish two cases for the parameter $c_3$, namely $c_3 \neq -1$ and $c_3 = -1$.

For $c_3 \neq -1$, we obtain for the function $B(t)$

$$\begin{aligned} B(t) &= \int_0^t D(s)\,\mathrm{d}s = \int_0^t c_1(1 + c_2 s)^{c_3}\,\mathrm{d}s = \frac{c_1}{c_2(c_3 + 1)}(1 + c_2 s)^{c_3+1}\Big|_0^t \\ &= \frac{c_1}{c_2(c_3 + 1)}[(1 + c_2 t)^{c_3+1} - 1] \end{aligned} \tag{23}$$

and, using equation (9),

$$n(t|D(t) = c_1(1 + c_2 t)^{c_3}) = \left[1 + E\frac{c_1}{c_2(c_3 + 1)}[(1 + c_2 t)^{c_3+1} - 1]\right]^{1/E}. \tag{24}$$

For $E = 0$ we obtain, using equation (13),

$$n(t|E = 0;\, D(t) = c_1(1 + c_2 t)^{c_3}) = \exp\left(c_1[(1 + c_2 t)^{c_3+1} - 1]/[c_2(c_3 + 1)]\right). \tag{25}$$

For $c_3 = -1$, we obtain for the function $B(t)$

$$B(t) = \int_0^t D(s)\,\mathrm{d}s = \int_0^t \frac{c_1}{1 + c_2 s}\,\mathrm{d}s = \frac{c_1}{c_2}\log_{\mathrm{e}}(1 + c_2 s)\Big|_0^t = \frac{c_1}{c_2}\log_{\mathrm{e}}(1 + c_2 t), \tag{26}$$

and for the growth function

$$n\left(t|D(t) = \frac{c_1}{c_2}\log_{\mathrm{e}}(1 + c_2 t)\right) = \left[1 + E\frac{c_1}{c_2}\log_{\mathrm{e}}(1 + c_2 t)\right]^{1/E} \tag{27}$$

and

$$n\left(t|E = 0;\, D(t) = \frac{c_1}{c_2}\log_{\mathrm{e}}(1 + c_2 t)\right) = \exp\left(\frac{c_1}{c_2}\log_{\mathrm{e}}(1 + c_2 t)\right) = (1 + c_2 t)^{c_1/c_2}. \tag{28}$$

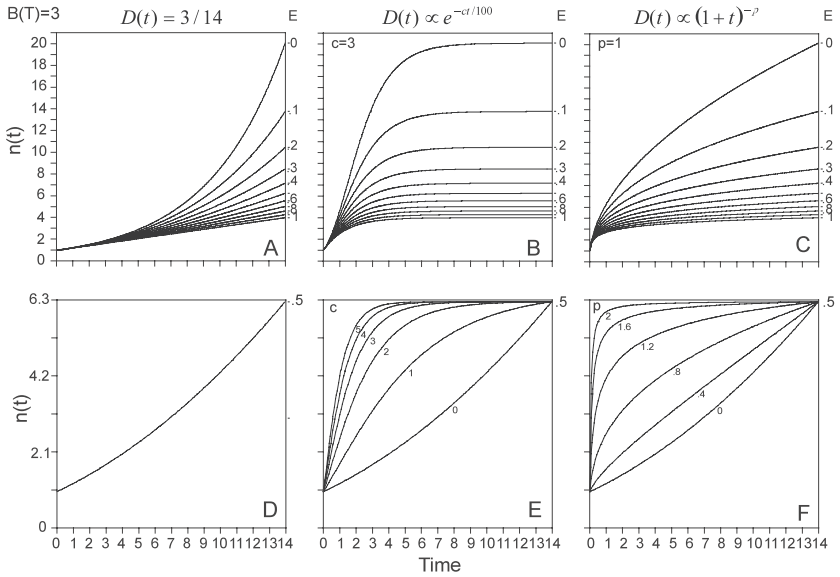


**Figure 3.** Growth functions for a range of values of the competition parameter $E$ and for constant (equations (16) and (17)), exponential (equations (20) and (21)), and power (equations (24), (25), (27), and (28)) functions for the baseline growth rate $D(t)$, calculated for a time range of 14 time units ($T = 14$). The growth functions in the upper row are calculated for a range of values of parameter $E$, and for a given parameter value in the different functions $D(t)$ with (A) a constant value of parameter $D$, (B) a given value of the coefficient $c$, and (C) a given value of the exponent $p$. The growth functions in the lower row are calculated for a range of values of the parameter in the different functions $D(t)$, and for a given value $E = 0.5$.

*2.4.6.* Examples of growth functions are given in figure 3, calculated for constant-$D$ conditions in 3(A), for exponential functions $D(t)$ in 3(B), and for power functions $D(t)$ in 3(C). The growth functions under constant-$D$ conditions (equations (16) and (17)) clearly show how the parameter $E$ controls the proliferation, ranging from a fully exponential increase for $E = 0$ (equation (17)) down to a linear increase for $E = 1$ (equation (16)). All the curves in figure 3(A), except the $E = 1$ one, show increasing derivatives with time, implying an acceleration of outgrowth, making constant-$D$ conditions unrealistic for dendritic outgrowth. The exponential $D$-functions (equations (20) and (21)) result in growth functions with clear asymptotic behaviour, with parameter $E$ controlling the asymptotic level. These properties make exponential $D$-functions appropriate candidates for describing dendritic growth as well as termination of growth. The power $D$-functions (equations (24), (25), (27), and (28)) also result in growth functions with decreasing growth rates but with less robust asymptotic behaviour, strongly dependent on parameter $E$. This makes power $D$-functions less suitable for describing termination of growth. In the following, we will study the growth functions under exponential $D$-functions. Constant-$D$ conditions are also explored because they are used in the analysis of experimental data, and they also illustrate the effect of proliferation on the growth function.

### *2.5. Growth functions for given boundary conditions with $E \neq 0$*

When the terminal segment number $n(T)$ at time $T$ is known we may express the growth function $n(t)$ and the baseline branching rate function $B(t)$ in these terms via equation (9) as

$$\frac{n^E(t) - 1}{n^E(T) - 1} = \frac{B(t)}{B(T)} \qquad \text{or} \qquad n(t) = \left[1 + (n^E(T) - 1)\frac{B(t)}{B(T)}\right]^{1/E} \tag{29}$$

or alternatively as

$$n(t) = n(T)\left[\frac{1 + EB(t)}{1 + EB(T)}\right]^{1/E} = n(T)\left[\frac{1/EB(T) + B(t)/B(T)}{1/EB(T) + 1}\right]^{1/E}. \quad (30)$$

For constant $D$ we have $\frac{B(t)}{B(T)} = \frac{t}{T}$, reducing equation (29) to

$$n(t|D) = \left[1 + (n^E(T) - 1)\frac{t}{T}\right]^{1/E}. \quad (31)$$

For exponential functions $D(t) = c_1 e^{c_2 t}$ we have, using (19), $\frac{B(t)}{B(T)} = (e^{c_2 t} - 1)/(e^{c_2 T} - 1)$, reducing equation (29) to

$$n(t|D(t) = c_1 e^{c_2 t}) = \left[1 + (n^E(T) - 1)\frac{e^{c_2 t} - 1}{e^{c_2 T} - 1}\right]^{1/E}. \quad (32)$$

### *2.6. Growth functions for given boundary conditions with $E = 0$*

For $E = 0$ we have, using equation (13),

$$\frac{n(t)}{n(T)} = e^{B(t)-B(T)} \qquad \text{or} \qquad n(t|E = 0) = n(T)e^{B(t)-B(T)}. \quad (33)$$

For constant $D$ we have $B(t) - B(T) = D(t - T)$, resulting in

$$n(t|E = 0; D) = n(T)e^{D(t-T)}. \quad (34)$$

For exponential functions $D(t) = c_1 e^{c_2 t}$ we have $B(t) - B(T) = \frac{c_1}{c_2}(e^{c_2 t} - e^{c_2 T})$, reducing equation (29) to

$$n(t|E = 0; D(t) = c_1 e^{c_2 t}) = n(T)\exp\left(\frac{c_1}{c_2}(e^{c_2 t} - e^{c_2 T})\right). \quad (35)$$

### *2.7. Terminal segment number distributions*

Under stochastic growth rules, trees experience varying numbers of branching events during the period of growth, resulting in a distribution for the terminal segment number of individual trees at a particular point in time. The mean of the distribution corresponds to the expressions for $n(t)$ as derived above. For the calculation of the variation in the distribution one needs to include all the possible growth sequences in a certain period of time. To calculate the distributions we use the following recurrent equation (Van Pelt *et al* 1997), here formulated in continuous time as

$$P_{tree}(n, t + \Delta t) = \sum_{j=0}^{n/2} P_{tree}(n - j, t)\binom{n - j}{j}[\bar{p}_s(t|n - j)\Delta t]^j[(1 - \bar{p}_s(t|n - j))\Delta t]^{n-2j} \quad (36)$$

with $P_{tree}(n, t)$ the probability of having a tree with $n$ terminal segments at time $t$ (with $P_{tree}(1, 0) = 1$), and $\bar{p}_s(t|n) = D(t)n^{-E}$ (equation (4)) denoting the mean branching probability per unit of time of a terminal segment in a tree with $n$ terminal segments. A tree of degree $n$ at time $t + \Delta t$ emerges when $j$ branching events occur at time $t$ in a tree of degree $n - j$. The recurrent equation expresses the probabilities of all these possible contributions from $j = 1, \ldots, n/2$. The last two terms express the probability that, in a tree of degree $n - j$, $j$ terminal segments will branch while the remaining $n - 2j$ terminal segments will not do so. The combinatorial coefficient $\binom{n-j}{j}$ expresses the number of possible ways of selecting

$j$ terminal segments from the existing $n - j$ ones. Note that the probability distribution of trees with varying terminal segment numbers is normalized at each time point $t$ and thus obeys

$$\sum_{n=1}^{n_{max}} P_{tree}(n,t) = 1, \qquad \forall t$$

with $n_{max}$ denoting the maximal possible terminal segment number at time $t$. Inserting the expression for $\bar{p}_s(t|n) = D(t)n^{-E}$ gives

$$P_{tree}(n,t+\Delta t) = \sum_{j=0}^{n/2} P_{tree}(n-j,t) \binom{n-j}{j} \times [D(t)(n-j)^{-E}\Delta t]^j [(1 - D(t)(n-j)^{-E}\Delta t)]^{n-2j} \tag{37}$$

which reduces for constant $D$ to

$$P_{tree}(n,t+\Delta t) = \sum_{j=0}^{n/2} P_{tree}(n-j,t) \binom{n-j}{j} [D(n-j)^{-E}\Delta t]^j \times [(1 - D(n-j)^{-E}\Delta t)]^{n-2j} \tag{38}$$

and for $E = 0$ to

$$P_{tree}(n,t+\Delta t) = \sum_{j=0}^{n/2} P_{tree}(n-j,t) \binom{n-j}{j} [D\,\Delta t]^j [1 - D\,\Delta t]^{n-2j}. \tag{39}$$

The distribution $P_{tree}(n,T)$ can now be obtained by calculating the distributions $P_{tree}(n,t)$ at all intermediate time points $t = \Delta t, 2\,\Delta t, 3\,\Delta t, \ldots, T$ with time steps $\Delta t$ taken equal to, for instance, one hour, and assuming that $P_{tree}(1,0) = 1$ and $P_{tree}(m,0) = 0, \forall m > 1$. An example is given in figure 4, illustrating the distributions obtained under the assumption of constant $D$ and for a time range [0–$T$] such that $B(T) = DT = 5$, and for several values of the parameter $E$. For instance, for a total time range of 14 days, $T = 14 \times 24 = 336$ h, $D = 5/336 = 0.0149$, and 336 iterations are needed for obtaining the final distribution.

For the special case $E = 0$, and taking $\Delta t = 1$, we obtain

$$P_{tree}(n,t+1) = \sum_{j=0}^{n/2} P_{tree}(n-j,t) \binom{n-j}{j} D^j (1-D)^{n-2j}. \tag{40}$$

Straightforward calculation of the recursion gives the following probability distributions for the first two time steps in table 1. It is easily verified that the probabilities meet the normalization criterion for each time point. The expected value for the number of terminal segments at time point $t = 2$ is now obtained via

$$\bar{n}(t=2) = \sum_{n=1}^{4} nP(n,t=2) = 1 + D^2$$

while the SD can be obtained via

$$\sigma_n(t=2) = \sqrt{\sum_{n=1}^{4} (n-\bar{n})^2 P(n,t=2)}.$$

Following this numerical approach we can calculate the mean and SD of the terminal segment number distributions for any combination of the parameters $B(T)$ and $E$. The results can compactly be visualized by mapping the ($B(T)$, $E$) parameter space onto the (mean, SD) space as shown in figure 5 (see also Van Pelt *et al* (1997)). This figure is a useful tool in finding those

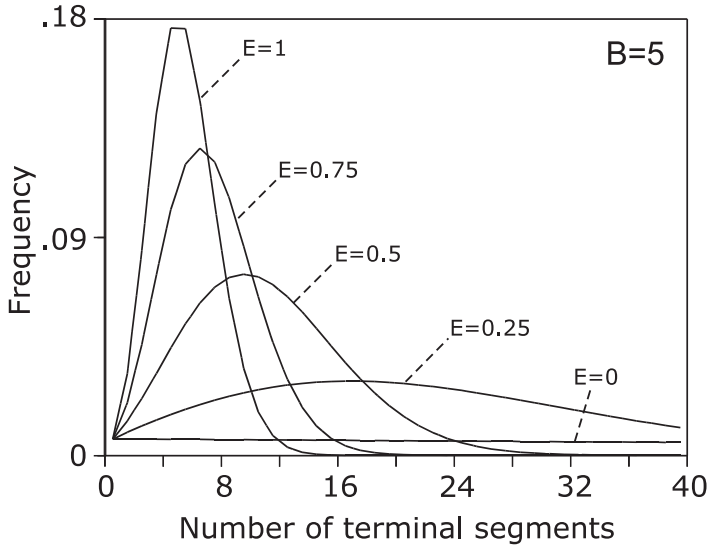


**Figure 4.** Frequency distributions of the terminal segment number of trees obtained after a period $T$ with $B(T) = 5$ and different values of the parameter $E$. Note that the mean and the width of the curves (SD) decrease with increasing values of the parameter $E$.

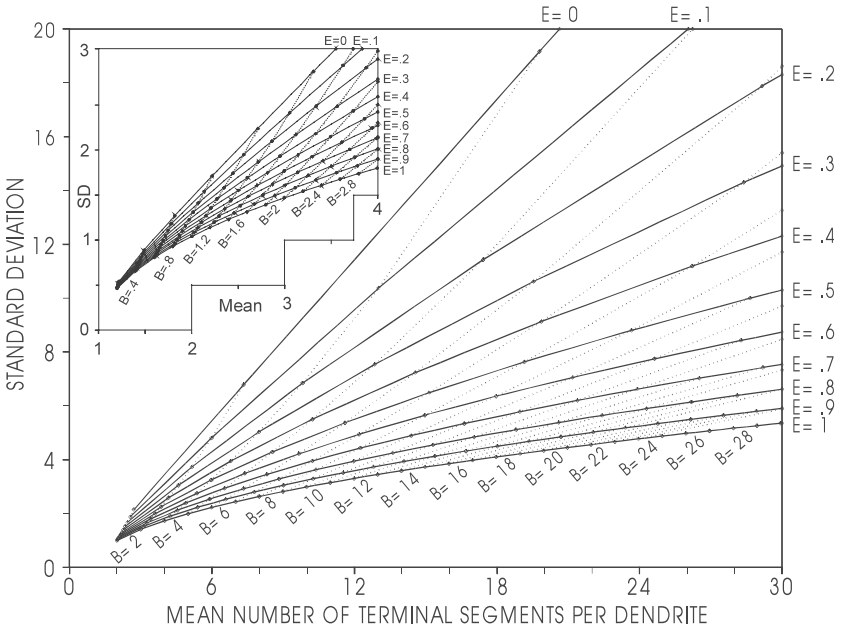


**Figure 5.** Mapping of the $(B(T), E)$ space onto the (mean, SD) space of the terminal segment number distributions. A continuous line connects (mean, SD) data points predicted for a particular value of parameter $E$. A dotted line connects (mean, SD) data points predicted for a particular value of parameter $B$. The inset shows the mapping in more detail for small values of the mean and SD.

values of the parameters $B(T)$ and $E$ that most optimally generate trees with similar mean and SD values for the terminal segment number distributions as has been observed.

**Table 1.** Probability $P_{tree}(n, t)$ at time $t$ of a tree with $n$ terminal segments for a branching process with constant $D$ and assuming $E = 0$.

| $t = 0$ | $t = 1$ | $t = 2$ |
|---|---|---|
| $P(1, 0) = 1$ | $P(1, 1) = 1 - D$ | $P(1, 2) = (1 - D)^2$ |
| | $P(2, 1) = D$ | $P(2, 2) = D(1 - D)(2 - D)$ |
| | | $P(3, 2) = 2D^2(1 - D)$ |
| | | $P(4, 2) = D^3$ |

According to equation (9), the expected number of terminal segments $n(t_i)$ at a particular point in time $t_i$ is a function of $B(t_i)$, implying that $n(t_i)$ at $t_i$ does not depend on the particular shape of the function $D(t)$ but on its time integral at $t_i$. Therefore, the relation between the parameter pair $(B(T), E)$ and the mean and SD of the terminal segment number distributions holds for any function $D(t)$, whose time integral at $T$ equals $B(T)$.

## 3. Analysis of experimental data

Different strategies will be explored to estimate the competition parameter $E$ and the baseline branching rate function $B(t)$ from experimental data, consisting of the mean and SD of the terminal segment number distributions at one or more points in time. These strategies will be illustrated using experimental data for dendritic trees of Wistar rat layer IV multipolar non-pyramidal neurons (table 2). These data originate from morphometrical studies on the growth of non-pyramidal neurons in the visual cortex of the rat (Parnavelas and Uylings 1980, Uylings *et al* 1980). The data obtained from 3D reconstructed Golgi–Cox stained neurons in coronal sections have been re-analysed in the present study in order to obtain the number of terminal segments of individual dendritic trees at the different developmental stages (4, 6, 8, 10, 12, 14, 16, 18, 20, 24, and 90 days postnatal). The coronal sectioning ensures that dendritic cutting, if occurring, is reduced to a minimum due to the finite thickness of the slices (120 $\mu$m). In the equations derived so far growth was assumed to start at $t = 0$. For the analysis of observed data the start time of growth will be denoted by $t_0$, and the time point after a period of growth $T$ will be denoted by $t_T$, thus with $T = t_T - t_0$. For the experimental data set used here, the start time of branching will be taken at $t_0 = 1$ day postnatal, being in the region of the end of the period of neuronal migration (Miller 1988) and the start of the backwards extrapolated growth curves for total number of segments and total dendritic length per neuron (Uylings *et al* 1994).

### *3.1. Estimation of parameters E and $B(t_T)$ from a single data point $(\bar{n}_{obs}(t_T), sd_{obs}(t_T))$ at time $t_T$*

A manual estimate of the parameters $E$ and $B(t_T)$ can be obtained using the family of curves in figure 5 by plotting the data point in the (mean, SD) frame and scoring the corresponding coordinates of the point in the $(B, E)$ frame. An automated optimization procedure is based on searching for those $(B, E)$ values that optimally predict the observed data. The choice of $(B, E)$ combinations in the search can be constrained by the relation, derived from equation (9),

$$n_{obs}(t_T) = [1 + EB(t_T)]^{1/E} \qquad \text{or} \qquad B(t_T) = \frac{n_{obs}^{E}(t_T) - 1}{E}. \tag{41}$$

That means that the search in the two-dimensional $(B, E)$ space can be reduced to a search in the one-dimensional $E$-space, by calculating for each choice of the parameter $E$ the corresponding value of parameter $B$. For each $(B, E)$ combination the terminal segment number distribution

**Table 2.** Observed values and model results for the mean and SD of the distributions of the terminal segment number of dendritic trees of Wistar rat layer IV multipolar non-pyramidal neurons at several development stages (4, 6, 8, 10, 12, 14, 16, 18, 20, 24, and 90 days). The experimental data originate from morphometrical studies on the growth of non-pyramidal neurons in the visual cortex of the rat (Parnavelas and Uylings 1980, Uylings *et al* 1980). The data from the coronal sections have been re-analysed in the present study in order to obtain the number of terminal segments of individual dendritic trees at the different developmental stages.

| Age | Observations | | | Model results | | | |
|---|---|---|---|---|---|---|---|
| (days) | No | Mean | SD | $B$ | $E$ | Mean | SD |
| 4 | 37 | 1.76 | 0.95 | 0.668 | 0.577 | 1.74 | 0.95 |
| 6 | 113 | 2.08 | 1.62 | 0.732 | 0.000 | 2.08 | 1.49 |
| 8 | 121 | 2.66 | 2.22 | 0.978 | 0.000 | 2.65 | 2.09 |
| 10 | 121 | 2.92 | 2.01 | 1.193 | 0.197 | 2.85 | 2.01 |
| 12 | 204 | 2.95 | 2.42 | 1.082 | 0.000 | 2.94 | 2.38 |
| 14 | 175 | 2.99 | 2.68 | 1.095 | 0.000 | 2.98 | 2.42 |
| 16 | 238 | 3.29 | 2.51 | 1.252 | 0.083 | 3.24 | 2.51 |
| 18 | 212 | 2.75 | 1.99 | 1.072 | 0.113 | 2.71 | 1.99 |
| 20 | 219 | 2.78 | 2.11 | 1.051 | 0.054 | 2.75 | 2.11 |
| 24 | 172 | 2.79 | 1.93 | 1.128 | 0.182 | 2.73 | 1.93 |
| 90 | 226 | 2.99 | 2.31 | 1.127 | 0.051 | 2.96 | 2.31 |
| | | | | | $\bar{E} = 0.114$ | | |

needs to be calculated using the recurrent equation (38) under the assumption of constant $D$, for obtaining the expected values for the mean and SD for this parameter set. Optimization ends when these expected values correspond optimally to the observed ones. The unknown growth function $n_{est}(t)$ can be expressed in terms of the optimized parameter values $(B_{opt}(t_T), E_{opt})$ using equation (29):

$$n_{est}(t) = \left[1 + (n_{obs}^{E_{opt}}(t_T) - 1)\frac{B(t)}{B_{opt}(t_T)}\right]^{1/E_{opt}}, \tag{42}$$

or, using equation (33),

$$n_{est}(t|E_{opt} = 0) = n_{obs}(t_T)\mathrm{e}^{B(t)-B_{opt}(t_T)} \tag{43}$$

for $E_{opt} = 0$. To make the growth function explicit we need to know the baseline branching rate function $D(t)$. When only one (mean, SD) data point is available, however, it is not possible to make any estimation. Examples of the course of the function $n(t)$ are given in figure 3 for three specific choices of the function $D(t)$. For instance, for constant $D$ we had $B(t) = \int_{t_0}^{t} D(s)\,\mathrm{d}s = D(t - t_0)$, which, given the value for $B_{opt}(t_T)$, becomes

$$D = \frac{B_{opt}(t_T)}{t_T - t_0}, \qquad \text{or} \qquad B(t) = B_{opt}(t_T)\frac{t - t_0}{t_T - t_0}. \tag{44}$$

By means of equation (42) we obtain

$$n_{est}(t|D) = \left[1 + (n_{obs}^{E_{opt}}(t_T) - 1)\frac{t - t_0}{t_T - t_0}\right]^{1/E_{opt}}, \tag{45}$$

or, using equation (34),

$$n_{est}(t|E_{opt} = 0;\, D) = n_{obs}(t_T)\mathrm{e}^{D(t-t_T)} = n_{obs}(t_T)\exp\left(B_{opt}(t_T)\left(\frac{t - t_T}{t_T - t_0}\right)\right) \tag{46}$$

resulting in a growth curve that will have one of the shapes displayed in figure 3(A).

In a similar way, growth functions for exponential $D(t)$ can be obtained from equation (32).

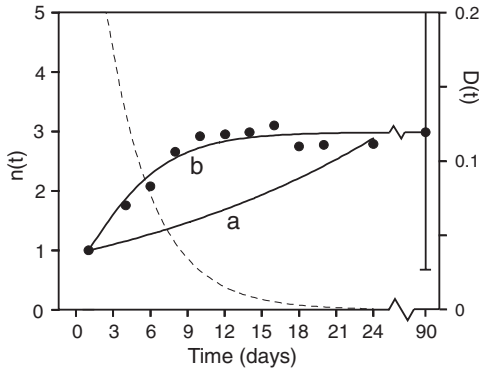


**Figure 6.** Model growth functions, estimated from the $\bar{n}_{obs}(90) = 2.99$, $sd_{obs}(90) = 2.31$ data point at $t = 90$ days. The curve (a) is obtained for a constant $D = 0.049$ function. The curve (b) is obtained by assuming an exponential function $D(t) = 0.398\mathrm{e}^{-0.27t}$ (dashed curve), of which the parameters have been optimized by fitting the resultant growth curve to the observed data at the other time points.

### *3.2. Estimation of the growth curve and baseline branching rate function D(t) from a series of data points* $(\bar{n}_{obs}(t_i), sd_{obs}(t_i))$ *at time points* $t_i (i = 1, \ldots, N)$

Four different approaches will be followed when data are available at more than one, say $N$, time points.

*3.2.1. Approach I.* In this approach we use one (mean, SD) data point, say at $t_i = t_T$, for estimation of $(B_{opt}(t_T), E_{opt})$ and use the other $N - 1$ data points for finding the baseline branching rate function $D_{est}(t)$. We follow the same approach as in the previous case for finding the optimized values $(B_{opt}(t_T), E_{opt})$ from the data point $(\bar{n}_{obs}(t_T), sd_{obs}(t_T))$ at time $t_T$. Subsequently, the baseline function $D_{est}(t)$ must be estimated such that the resultant growth function $n_{est}(t)$ according to equation (42) runs optimally through the other experimental data points $\bar{n}_{obs}(t_i)$ at time points $t_i$.

For an exponential function $D(t) = c_1\mathrm{e}^{c_2 t}$ the estimated growth function becomes (equation (32))

$$n_{est}(t|c_2) = \left[1 + (n^E_{obs}(t_T) - 1)\frac{\mathrm{e}^{c_2(t-t_0)} - 1}{\mathrm{e}^{c_2 T} - 1}\right]^{1/E_{opt}}. \tag{47}$$

**Example I.** Using the $t = 90$ days data point $\bar{n}_{obs}(90) = 2.99$, $sd_{obs}(90) = 2.31$ from table 2, an estimate is obtained for the growth parameters $B_{opt}(90) = 1.127$ and $E_{opt} = 0.051$. With these values, and assuming $t_0 = 1$ (i.e., growth starts with one unbranched segment at one day postnatal), thus $T = t_T - t_0 = 89$, the estimated growth function becomes $n_{est}(t|c_2) = [1 + 0.057(\mathrm{e}^{c_2(t-1)} - 1)/(\mathrm{e}^{c_2 89} - 1)]^{19.6}$. A best estimate $c_2 = -0.27$ is now obtained after fitting the function to the data at the other time points, such that the estimated growth function reduces to $n_{est}(t) = 2.96[1 - 0.071\mathrm{e}^{-0.27t}]^{19.6}$, as displayed in figure 6. A best estimate $c_1 = 0.304$ is obtained using equation (19) and the optimized value $B_{opt}(90) = 1.127$, yielding an estimate for the baseline branching rate function $D(t) = 0.304\mathrm{e}^{-0.27(t-1)} = 0.398\mathrm{e}^{-0.27t}$.

*3.2.2. Approach II.* In this approach the observed growth function is first approximated by some best-fitting analytical expression $n_{fit}(t)$ through the data points. Secondly, the

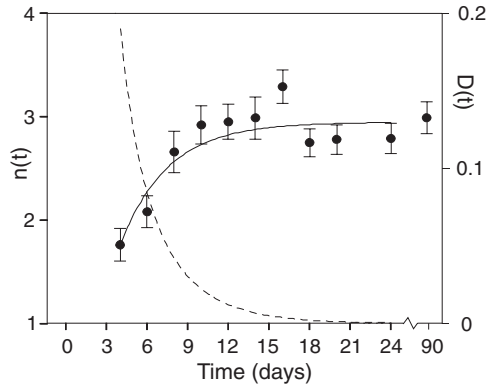


**Figure 7.** The mean and standard error (dots and bars, respectively) of the terminal segment number distributions of dendritic trees at several time points during their outgrowth up to their mature branching patterns. The solid line represents the fitted function $n_{fit}(t) = 2.95 - 3.74\mathrm{e}^{-0.29t}$ through these data points. The dashed curve represents the baseline branching rate function $D_{est}(t) = 0.416\mathrm{e}^{-0.29t}[1 - 1.27\mathrm{e}^{-0.29t}]^{-0.886}$, derived from the fitted function $n_{fit}(t)$.

time course of the baseline branching rate function $D(t)$ is approximated using the following expression, derived from equation (5):

$$D_{est}(t) = n_{fit}^{E-1}\frac{\mathrm{d}n_{fit}(t)}{\mathrm{d}t}. \tag{48}$$

For this approach we need also an estimate of the parameter $E$. When at different time points both experimental values for the mean and SD are available, we may estimate at each time point $t_i$ values for $E_{est}(t_i)$ and $B_{est}(t_i)$. The values $B_{est}(t_i)$ are expected to increase during the growth process as reflecting the increasing integral number of expected branching events by the baseline branching process. The values $E_{est}(t_i)$ in contrast are expected to remain constant assuming a constant and sustained underlying 'competitive process'. Then, $E_{est}$ can be taken as the mean over all the time points.

**Example II.** Approximating the observed values for the mean number of terminal segments at different points in time during development (third column in table 2) by an exponential function yields a best-fitting function

$$n_{fit}(t) = 2.95 - 3.74\mathrm{e}^{-0.29t}.$$

Using equation (48) the function $D_{est}(t)$ can then be estimated by

$$D_{est}(t) = n_{fit}^{E-1}(t)\frac{\mathrm{d}n_{fit}(t)}{\mathrm{d}t} = [2.95 - 3.74\mathrm{e}^{-0.29t}]^{E-1}1.085\mathrm{e}^{-0.29t}.$$

Estimated values of $E$ for each time point are given in the sixth column of table 2, having a mean value of $\bar{E} = 0.114$ which makes the function $D_{est}(t)$ explicit as

$$D_{est}(t) = 0.416\mathrm{e}^{-0.29t}[1 - 1.27\mathrm{e}^{-0.29t}]^{-0.886}.$$

The best-fitting growth function and the baseline branching rate function $D_{est}(t)$ are displayed in figure 7.

*3.2.3. Approach III.* Here we approximate the function $D(t)$ by means of a time transformation. First, we estimate $(B_{opt}(t_T), E_{opt})$ for one of the data points (e.g., from $\bar{n}_{obs}(t_T)$ and $sd_{obs}(t_T)$ at time $t_T$), and calculate the growth function assuming constant $D$ using equation (31):

$$n_{est}(t|D) = \left[1 + (\bar{n}_{obs}^{E_{opt}}(t_T) - 1)\frac{t - t_0}{T}\right]^{1/E_{opt}} \tag{49}$$

or

$$n_{est}(t|E_{opt} = 0;\, D) = \bar{n}_{obs}(t_T)\mathrm{e}^{D(t-t_T)} \tag{50}$$

for $E_{opt} = 0$. Second, for each of the other observed data points we determine at which time point the calculated function attains a similar value. Then we construct a mapping of these time points of the calculated growth function to their corresponding observed time points, and calculate the best-fitting transformation function $t \to F(t)$. When we insert this time mapping into equation (49) we obtain

$$n_{fit}(t) = \left[1 + (\bar{n}_{obs}^{E_{opt}}(t_T) - 1)\frac{F(t) - t_0}{T}\right]^{1/E_{opt}}. \tag{51}$$

This fitted function should run optimally through the observed data points. When comparing equation (51) with (42) we obtain an estimate for the unknown function $B_{est}(t)$ via

$$B(t) = B(t_T)\frac{F(t) - t_0}{T}. \tag{52}$$

The function $D_{est}(t)$ can be obtained via equation (10):

$$D_{est}(t) = \frac{\mathrm{d}}{\mathrm{d}t}B_{est}(t) = \frac{B_{opt}(t_T)}{T}\frac{\mathrm{d}F(t)}{\mathrm{d}t}. \tag{53}$$

**Example III.** We will restrict this example to the initial growth phase $t = 1$–$14$ days, with, $n(t_0) = 1$, $t_T = 14$, and $n(t_T) = 2.99$, and thus with $T = 13$. From the terminal segment number mean and SD at day 14 the parameter values $E = 0.0$ and $B = 1.10$ have been derived (table 2). With these growth parameters a growth curve can be drawn using equation (34). Assuming constant $D$, we have $D = B/T = 1.1/13 = 0.085$, and the growth curve becomes

$$n_{est}(t|E = 0;\, D = 0.085) = 2.99\mathrm{e}^{0.085(t-t_T)}$$

when time is expressed in days and has been drawn in figure 8(A). When the time points of the observations are related to the time points at which the growth curve attains similar values we obtain a mapping as given in figure 8(B). This time mapping can be approximated by the regular function $F(t) = 15.3 - 17.8\mathrm{e}^{-0.21t}$. Replacing time $t$ by the function $F(t)$, $t \to F(t)$, results in a model growth function

$$n_{fit}(t) = 2.99\mathrm{e}^{0.085(15.3-17.8\mathrm{e}^{-0.21t}-14)} = 3.3\mathrm{e}^{-1.5\mathrm{e}^{-0.21t}},$$

which is drawn in figure 8(C) and now runs smoothly through the observed data points. Note that also the model-predicted SD values now nicely agree with the observed SD values. For the function $D_{est}(t)$ we obtain (equation (53))

$$D_{est}(t) = \frac{B_{opt}(T)}{T}\frac{\mathrm{d}F(t)}{\mathrm{d}t} = 0.315\mathrm{e}^{-0.21t}$$

as drawn in figure 8(D). This result illustrates how the baseline branching probability rapidly decreases with time. Although other functions may be chosen as well to approximate the time mapping, they will all result in a general decreasing behaviour of the function $D(t)$.

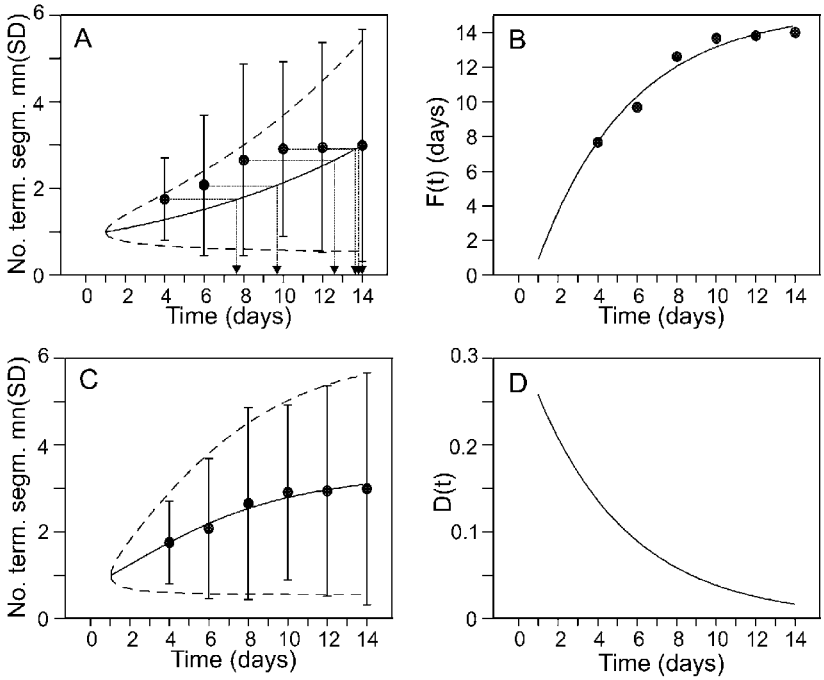


**Figure 8.** (A) Mean (dots) and SD (bars) of the observed terminal segment numbers in the first days of dendritic outgrowth. The model growth curve mean (solid curve) and SD (dashed curves) are calculated using the recurrent equation (39) for $E = 0$ and constant $D = 0.085$, estimated from the $t = 14$ data point and taking $t_0 = 1$ as the start of the branching process. The thin lines relate the time points of observations with the time points at which the model curve attains similar values. These time relations are plotted in (B) as dots through which a best-fitting curve $F(t) = 15.3 - 17.8\mathrm{e}^{-0.21t}$ is drawn. (C) A similar plot to (A), but with the model curves drawn against a transformed timescale according to the function $F(t)$ displayed in (B). (D) The baseline branching rate function $D_{est}(t) = 0.315\mathrm{e}^{-0.21t}$, obtained from the time-transformed model growth curve.

*3.2.4. Approach IV.* In this approach we first estimate values for $B_{opt}(t_i)$ and $E_{opt}(t_i)$ for each time point $t_i$. Assuming $E$ to be constant during the whole growth process we then obtain an estimate of $E$ by taking the average of these individual estimates:

$$\bar{E}_{est} = \frac{1}{N}\sum_{i=1}^{N} E_{est}(t_i).$$

An approximation of the function $B(t)$ can be obtained by finding a smooth function $B_{est}(t)$ through the individual estimated values $B_{opt}(t_i)$. An estimate for the function $D(t)$ is then obtained by taking the derivative of $B_{opt}(t_i)$:

$$D_{est}(t) = \frac{\mathrm{d}}{\mathrm{d}t} B_{est}(t).$$

**Example IV.** The optimized $E$-values in table 2 result in an average of $\bar{E} = 0.114$. The values of $B(t_i)$ are plotted in figure 9 and approximated by the function $B(t) = a + b\mathrm{e}^{cx}$, with $a = 1.14$, $b = -1.72$, and $c = -0.3$. The baseline branching rate function can now be estimated by taking the time derivative of this function $B(t)$, resulting in the dashed curve $D(t) = 0.52\mathrm{e}^{-0.3t}$.

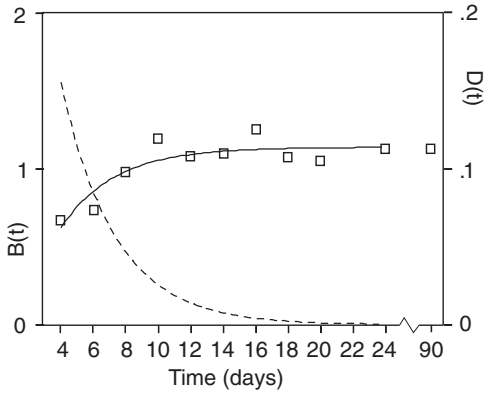


**Figure 9.** Individual data points $B(t_i)$ (squares), derived from the observed (mean, SD) values of the terminal segment numbers for successive days of observation (table 2). The solid curve represents a best-fitting function $B(t) = 1.14 - 1.72\mathrm{e}^{-0.3x}$. The dashed curve represents the derivative function $D(t) = 0.52\mathrm{e}^{-0.3t}$.

## 4. Summary and discussion

During outgrowth, dendritic trees increase their number of terminal segments by a sequence of branching events. The dendritic growth rate, i.e., the rate of increase of the terminal segment number, therefore depends on this increasing number as well as on the branching probability of the individual terminal segments. In this paper, a method has been described for extracting the mean branching probability from the dendritic growth rate. Moreover, it is shown how this branching probability can be decomposed into a component depending on the momentary number of terminal segments in the tree ('competition effect') and a 'baseline' component representing all other factors. This decomposition is based on the specific relation between the mean and the SD of the terminal segment number distributions. The contribution of these two components to the dendritic growth rate has been made explicit using a model-based approach. Assuming a power dependence of the branching probability on the terminal segment number (with exponent $-E$), it was possible to relate explicitly the time course of the baseline branching rate to the dendritic growth rate. By means of these relations it was shown how the time course of the baseline branching rate could be estimated from the mean and SD of the terminal segment number distributions, experimentally obtained from dendrites of Wistar rat cortical multipolar non-pyramidal neurons at several developmental stages. The method has been illustrated using four different estimation approaches, with the results summarized in table 3, and shown graphically in figure 10.

These results underscore the main finding that the baseline branching rate is a rapidly and monotonically decreasing function of time. This result is in combination with the non-zero mean value of the competition parameter $E = 0.114$. Apparently, the branching probability of a terminal segment during dendritic outgrowth not only decreases over time because of the competitive effect of the proliferating number of terminal segments, but also because of a baseline factor, not related to a competitive effect. The time course of the mean branching probability of a terminal segment can be obtained by inserting the functions $D(t)$ and $n(t)$ with the value $E = 0.114$ into equation (4). In the case of approach I we obtained $D(t) = 0.398\mathrm{e}^{-0.27t}$ and $n_{est}(t) = 2.96[1 - 0.071\mathrm{e}^{-0.27t}]^{19.6}$, resulting in an estimated branching probability function $p(t) = D(t)n_{est}^{-E}(t) = 0.352\mathrm{e}^{-0.27t}[1 - 0.071\mathrm{e}^{-0.27t}]^{-2.234}$.

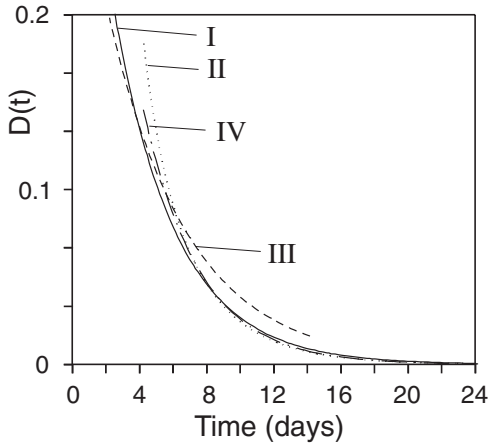


**Figure 10.** The time course of the baseline branching rate during outgrowth of dendrites of multipolar non-pyramidal neurons, estimated using four different approaches, from the mean and SD of the dendritic tree terminal segment number distributions for several days of dendritic development. The ordinate range has been limited to 0.2 to remain close within the time range of observed data points (table 2).

**Table 3.** Estimation of the baseline branching rate function $D(t)$ from the observed mean–SD values of the terminal segment numbers of Wistar rat layer IV multipolar non-pyramidal neuron dendritic trees obtained at different time points during their development to mature trees. The table lists the results obtained using the four different approaches.

| Method | Time range used for estimation (days) | Estimated baseline branching rate function $D(t)$ |
|---|---|---|
| I | [1–90] | $0.398\mathrm{e}^{-0.27t}$ |
| II | [4–90] | $0.416\mathrm{e}^{-0.29t}[1 - 1.27\mathrm{e}^{-0.29t}]^{-0.886}$ |
| III | [1–14] | $0.315\mathrm{e}^{-0.21t}$ |
| IV | [4–90] | $0.52\mathrm{e}^{-0.3t}$ |

Thus, starting with a branching probability per day of $p(0) \approx 0.4$ at day zero, it drops down to $p(10) \approx 0.02$ at day 10 and $p(20) \approx 0.0016$ at day 20.

The four methods differ in the estimation approach and in the use of experimental data, consisting of means and SDs of the terminal segment number in dendritic trees at different time points. Method I uses the mean and SD value at one time point $T$ to estimate the growth parameters $E$ and $B(T)$, and the mean values at all other time points to fit the growth function, assuming an exponential baseline branching rate function. Method II uses the mean values at all time points to find a best-fitting growth function. The baseline branching rate function is obtained from this growth function using an estimate of the competition parameter $E$ taken as the mean of the $E$-estimates for the individual data points. Method III uses the mean and SD value at one time point to estimate the growth parameters for drawing the growth curve assuming a constant baseline branching rate $D$. As this growth curve likely deviates from the observed one, a mapping is constructed between the time points at which the model curve and the observed data points attain similar values. A best-fitting time-transformation function through this mapping is subsequently applied to the model growth curve from which finally the baseline branching rate function is derived. Method IV uses the mean and SD values at all time points to estimate the growth parameters $B(t_i)$ and $E(t_i)$ at each individual time point

$t_i$. An estimate of the competition parameter $E$ is obtained by averaging the individual $E(t_i)$ values. The baseline branching rate function $D(t)$ is estimated by taking the derivative of a best-fitting curve through the individual $B(t_i)$ values. The outcomes of the four methods differ only slightly in the detailed shape of the baseline branching rate functions (table 3, figure 10), indicating that the general behaviour is highly robust. In all four methods curve fitting has been applied, with exponential functions for the baseline branching rate function (method I), the growth function (method II), the time transformation (method III), and the $B$-function (method IV) turning out to give satisfactory fits. Although other functions could have been applied as well, they will not result in other conclusions. As the four methods appear comparable in their performance, no general preference can be given. However, the choice of method may depend on the type of experimental data that are available. For instance, if SD values are not available at all time points, method I or method III may be the choice. If the start time of the branching process is unknown, method II or method IV may be the choice. If data are available at only a few time points, method I may be used. If one does not like the use of best-fitting functions, one may use method III, and replace the best-fitting time-transformation function by a piecewise-linear interpolation, resulting in a non-continuous differentiable estimate of the baseline branching rate curve (see for instance figure 7 in Van Pelt *et al* (1997)).

*Topological implications.* In this study we have focused on the branching process and the rate of increase of the number of terminal segments. A similar model of branching, but with constant, time-independent branching probabilities, has been studied by Horsfield *et al* (1987) for its consequences on topological properties of the resultant trees. This study made explicit predictions for the ratio of the number of different types of branch point, i.e. those leading to two terminal segments (primary vertices $V_a$), and those leading to a terminal and an intermediate segment (secondary vertices $V_b$). These authors showed that, for large trees, the vertex ratio $V_b/V_a$ relates directly to the absolute branching probability of terminal segments $p_{syn}$ according to $V_b/V_a = 1-p_{syn}$. Our analysed data set, however, concerned small dendritic trees, while the mean branching probability was not constant but a rapidly decreasing function of time from a value of about 0.4 at day zero down to 0.0016 at day 20. Conclusions concerning the expected value for the $V_b/V_a$ ratio thus are not directly being made. Nevertheless, the rapid decline of the branching probability may result in a vertex ratio close to one, which would be compatible with a mode of random terminal growth (Verwer and Van Pelt 1985), and with the value of 0.47 for the tree asymmetry index obtained from the 16 DIV group in the sample studied, which value is compatible with the expected value for this mode of growth (Van Pelt *et al* 1992).

In conclusion, this study has shown how primary characteristics of dendritic tree terminal segment number distributions (mean and SD) at different developmental stages can be used to investigate details of the branching process, including the time course of branching of individual growth cones, the influence of their increasing number (competition), and the time course of the baseline branching rate function. The question of what these details tell us about the cellular and molecular mechanisms involved in dendritic branching and growth cone behaviour requires further experimental and computational investigation.

## References

Ascoli G 2002 Neuroanatomical algorithms for dendritic modeling *Network: Comput. Neural Syst.* **13** 247–60 (this issue)

Ascoli G and Krichmar J L 2000 L-neuron: a modeling tool for the efficient generation and parsimonious description of dendritic morphology *Neurocomputing* **32–3** 1003–11

Bray D 1973 Branching patterns of individual sympathetic neurons in culture *J. Cell Biol.* **56** 702–12

Burke R E, Marks W B and Ulfhake B 1992 A parsimonious description of motoneuron dendritic morphology using computer simulation *J. Neurosci.* **12** 2403–16

Dityatev A E, Chmykhova M, Studer L, Karamian O A, Kozhanov V M and Clamann H P 1995 Comparison of the topology and growth rules of motoneuronal dendrites *J. Comput. Neurol.* **363** 505–16

Horsfield K, Woldenberg M J and Bowes C L 1987 Sequential and synchronous growth models related to vertex analysis and branching ratios *Bull. Math. Biol.* **49** 413–29

Juraska J M 1982 The development of pyramidal neurons after eye opening in the visual cortex of hooded rats: a quantitative study *J. Comput. Neurol.* **212** 208–13

Miller M W 1988 Development of projection and local circuit neurons in neocortex *Development and Maturation of Cerebral Cortex* vol 7, ed A Peters and E G Jones (New York: Plenum) pp 133–75

Nowakowski R S, Hayes N L and Egger M D 1992 Competitive interactions during dendritic growth: a simple stochastic growth algorithm *Brain Res.* **576** 152–6

Parnavelas J G and Uylings H B M 1980 The growth of non-pyramidal neurons in the visual cortex of the rat: a morphometric study *Brain Res.* **193** 373–82

Pentney R 1986 Quantitative analysis of dendritic networks of Purkinje neurons during aging *Neurobiol. Aging* **7** 241–8

Petit P L, LeBoutillier J C, Gregorio A and Libstug H 1988 The pattern of dendritic development in the cerebral cortex of the rat *Dev. Brain Res.* **41** 209–19

Sadler M and Berry M 1984 Remodeling during development of the Purkinje cell dendritic tree in the mouse *Proc. R. Soc.* B **221** 349–68

Uylings H B M, Parnavelas J G, Walg H and Veltman W A M 1980 The morphometry of the branching pattern of developing non-pyramidal neurons in the visual cortex of rats *Mikroskopie* **37** 220–4

Uylings H B M, Ruiz-Marcos A and Van Pelt J 1986 The metric analysis of three-dimensional dendritic tree patterns: a methodological review *J. Neurosci. Methods* **18** 127–51

Uylings H B M, Smit G J and Veltman W A M 1975 Ordering methods in quantitative analysis of branching structures of dendritic trees *Adv. Neurol.* **12** 247–54

Uylings H B M, Van Pelt J, Parnavelas J G and Ruiz-Marcos A 1994 Geometrical and topological characteristics in the dendritic development of cortical pyramidal and non-pyramidal neurons *The Self-Organizing Brain: from Growth Cones to Functional Networks (Progress in Brain Research vol 102)* ed J van Pelt, M A Corner, H B M Uylings and F H Lopes da Silva (Amsterdam: Elsevier)

Van Ooyen A 2001 Competition in the development of nerve connections: a review of models *Network: Comput. Neural Syst.* **12** R1–47

Van Ooyen A, Graham B P and Ramakers G J A 2001 Competition for tubulin between growing neurites during development *Neurocomputing* **38–40** 73–8

Van Pelt J, Dityatev A E and Uylings H B M 1997 Natural variability in the number of dendritic segments: model-based inferences about branching during neurite outgrowth *J. Comput. Neurol.* **387** 325–40

Van Pelt J, Schierwagen A and Uylings H B M 2001 Modeling dendritic morphological complexity of deep layer cat superior colliculus neurons *Neurocomputing* **38–40** 403–8

Van Pelt J and Uylings H B M 1999a Modeling the natural variability in the shape of dendritic trees: application to basal dendrites of small rat cortical layer 5 pyramidal neurons *Neurocomputing* **26–7** 305–11

Van Pelt J and Uylings R W H 1999b Natural variability in the geometry of dendritic branching patterns *Modeling in the Neurosciences—from Ionic Channels to Neural Networks* ed R R Poznanski (Amsterdam: Harwood) pp 79–108

Van Pelt J, Uylings H B M, Verwer R W H, Pentney R J and Woldenberg M J 1992 Tree asymmetry—a sensitive and practical measure for binary topological trees *Bull. Math. Biol.* **54** 759–84

Van Pelt J, Van Ooyen A and Uylings H B M 2000 Modeling dendritic geometry and the development of nerve connections *Computational Neuroscience, Realistic Modeling for Experimentalists* ed E de Schutter and R C Cannon (Boca Raton, FL: CRC Press) pp 179–208

Van Pelt J and Verwer R W H 1986 Topological properties of binary trees grown with order-dependent branching probabilities *Bull. Math. Biol.* **48** 197–211

Verwer R W H and Van Pelt J 1985 Topological analysis of binary tree structures when occasional multifurcations occur *Bull. Math. Biol.* **47** 305–16

Woldenberg M J, O'Neill M P, Quackenbush L J and Pentney R J 1993 Models for growth, decline and regrowth of the dendrites of rat Purkinje cells induced from magnitude and link-length analysis *J. Theor. Biol.* **162** 403–29